Phase diagram of classical electronic bilayers

2006 J. Phys. A: Math. Gen. 39 4595

(http://iopscience.iop.org/0305-4470/39/17/S44)

INSTITUTE OF PHYSICS PUBLISHING JOURNAL OF PHYSICS A: MATHEMATICAL AND GENERAL

J. Phys. A: Math. Gen. **39** (2006) 4595–4600 doi:10.1088/0305-4470/39/17/S44

Phase diagram of classical electronic bilayers

S Ranganathan[1] **and R E Johnson**[2]

[1] Department of Physics, Royal Military College of Canada, Kingston, Ontario K7K 7B4, Canada
[2] Department of Mathematics and Computer Science, Royal Military College of Canada, Kingston, Ontario K7K 7B4, Canada

Received 31 August 2005, in final form 8 November 2005
Published 7 April 2006
Online at stacks.iop.org/JPhysA/39/4595

Abstract

Extensive molecular dynamics calculations have been performed on classical, symmetric electronic bilayers at various values of the coupling strength Γ and interlayer separation d to delineate its phase diagram in the Γ–d plane. We studied the diffusion, the amplitude of the main peak of the intralayer static structure factor and the peak positions of the intralayer pair correlation function with the aim of defining equivalent signatures of freezing and constructing the resulting phase diagram. It is found that for Γ greater than 75, crystalline structures exist for a certain range of interlayer separations, while liquid phases are favoured at smaller and larger d. It is seen that there is good agreement between our phase diagram and previously published ones.

PACS numbers: 61.20.Ja, 52.27.Gr, 52.65.Yy

1. Introduction

A one-component plasma (OCP), a system of classical electrons interacting with a $1/r$ potential in the presence of a uniform neutralizing background, is one of the simplest models used to study electronic motion in two and three dimensions. Properties of such systems depend only on one parameter, the classical coupling strength $\Gamma = \frac{e^2}{ak_BT}$ which is the ratio of the average potential energy to the average kinetic energy per particle; a is the interparticle distance equal to $(3/4n\pi)^{1/3}$ in three dimensions and $(1/n\pi)^{1/2}$ in two dimensions, with n being the particle density. Bilayers, consisting of two plane layers of charged particles, represent the simplest form of multilayered systems. Properties of such systems depend on an additional parameter, the interlayer separation d; this causes the system to exhibit a rich variety of structural and dynamical behaviour. Since layered structures of charged particles can now be realized in various physical systems such as ion traps and semiconductor devices; bilayers have become a focus of experimental [1, 2], theoretical [3, 4] and computer simulation [5–9] investigations.

Molecular dynamics simulations [6] for a bilayer with a high value of Γ have revealed the presence of solid phases at intermediate d, even though the system is in a fluid phase at small and large d. This additional degree of freedom (the interlayer separation d) enhances

the interlayer correlations and seems to stabilize crystalline structures for certain values of d. Thus, it is of interest to study this richer phase diagram and delineate the solid–fluid transition line in the entire Γ–d plane. Calculations based on diffusion Monte Carlo technique [10] and on Monte Carlo simulations [11] have resulted in a phase diagram for a symmetric electron bilayer. In [11], the authors have analysed changes in the potential energy of a classical system to obtain the phase diagram, while in [10], the authors have looked at the ground state energy of quasi-quantum spin system. In this paper, we focus on a measurable property of the system, the diffusion coefficient, to determine the phase diagram. In addition, we look at the peak values of the intralayer static structure factor $S_{11}(q)$ to see if they are consistent with a suggested universal criterion of freezing.

2. Simulation details

The system to be simulated is a bilayer consisting of classical electrons interacting through a $1/r$ Coulomb potential. The electrons are distributed in two planes separated by a constant distance d; each electron is constrained to move only in the plane of its original distribution. Charge neutrality is guaranteed by embedding the electrons in a uniform background of the opposite charge. Only symmetric bilayers, in which the density of the electrons is the same in both layers, are considered in this study.

The details of the simulation and the extended Ewald sum technique have been described in our earlier papers [12], but for the sake of completeness, we include some of the essential features here. The dynamics in our MD simulation needs the force and, as an example, the force on any one particle due to all particles in the same plane and the other plane is given by

$$\begin{aligned}\vec{F}(\vec{r}_1) = \frac{2\pi}{L^2}\sum_{\vec{g}\neq\vec{0}}\vec{g}\left\{\frac{1}{g}\operatorname{erfc}\left(\frac{g}{2\alpha}\right)\sum_{j=2}^{N}\sin[\vec{g}\circ(\vec{r}_1-\vec{r}_j)]+\psi(g;\kappa,d)\sum_{j=1}^{N}\sin[\vec{g}\circ(\vec{r}_1-\vec{\rho}_j)]\right\}\\ +{\sum_{\vec{p}}}'\sum_{j=1}^{N}\frac{\vec{s}_{1j}}{|\vec{s}_{1j}|^3}\left\{\operatorname{erfc}(\alpha|\vec{s}_{1j}|)+\alpha|\vec{s}_{1j}|\frac{2}{\sqrt{\pi}}\exp(-\alpha^2|\vec{s}_{1j}|^2)\right\}\\ +\sum_{\vec{p}}\sum_{j=1}^{N}\frac{\vec{d}_{1j}}{|\vec{d}_{1j}|^3}\left\{\operatorname{erfc}(\kappa|\vec{d}_{1j}|)+\kappa|\vec{d}_{1j}|\frac{2}{\sqrt{\pi}}\exp(-\kappa^2|\vec{d}_{1j}|^2)\right\}\end{aligned} \tag{1}$$

with

$$\begin{aligned}\psi(g;\kappa,d)&=\int_0^\infty \mathrm{d}r\,\frac{r}{\sqrt{r^2+d^2}}\operatorname{erf}\left(\kappa\sqrt{r^2+d^2}\right)J_0(gr)\\ &=\frac{1}{2g}\left[e^{gd}\operatorname{erfc}\left(\frac{g}{2\kappa}+\kappa d\right)+e^{-gd}\operatorname{erfc}\left(\frac{g}{2\kappa}-\kappa d\right)\right],\end{aligned} \tag{2}$$

$\vec{s}_{1j}=\vec{r}_1-\vec{r}_j+\vec{p}$ and $\vec{d}_{1j}=\vec{r}_1-\vec{\rho}_j+\vec{d}+\vec{p}$; $\vec{r}_i$ denotes the position of the ith electron in the same (x, y) plane and $\vec{\rho}_j$ is the position of the jth electron in the other (x, y) plane, and the planes are separated by a distance d along the z-axis; L is the length of the square simulation cell and N is the number of electrons in each cell. The sum over $\vec{p}$ is a sum over integers k_1, k_2 with $\vec{p}=L(k_1,k_2)$; the prime on this sum implies that if $j=1$, the $\vec{p}=\vec{0}$ term is to be omitted. The sum over $\vec{g}$ is a sum over integers λ_1, λ_2 with $\vec{g}=\frac{2\pi}{L}(\lambda_1,\lambda_2)$. The parameters α and κ are to be chosen so that both series in (1) converge rapidly. Our studies have indicated that a good choice for both of the parameters is $8/L$ and an acceptable accuracy can be obtained using $\sqrt{45}$ for the largest $|\vec{\lambda}|$; this corresponds to taking 78 terms in the g-space sums in the expression for the force. This is sufficiently large that only the

$\vec{p} = \vec{0}$ terms in the r-space summation in (1) need to be retained, implying that the real-space term vanishes at a distance corresponding to the distance from the cell centre to its edge. All quantities involved are in dimensionless units: distance in units of WS radius a, time in units of $\tau = \sqrt{\frac{ma^3}{e^2}}$. The two layers have the same surface density and the basic cell is a square with side length $L = \left(\frac{N}{na^2}\right)^{1/2}$, containing 512 electrons in each of the two layers. Since a is the unit of length, the density in each layer takes the value $1/\pi$. The time step for the dynamics (Verlet algorithm) was chosen to be 0.03 in dimensionless units. The temperature scaling is done every 50 steps until the system can maintain the temperature without the scaling. We were able to keep the temperature T to within 2% of the desired temperature in each layer. Γ is just the reciprocal of the temperature in dimensionless units. Our MD data consist of the position vector $\vec{r}_k(t) = [x_k(t), y_k(t)]$ and the velocity vector $\vec{v}_k(t) = [v_{kx}(t), v_{ky}(t)]$ for $k =$ 1–512 particles and for 10 000 times separated by a time step of 0.06. These data are then used to obtain the various correlation functions. Simulations were performed for values of Γ from 20 to 120 and d from 0.1 to 3.0.

3. Results

After the MD data for the position vector and the velocity vector have been generated for a specific value of the coupling parameter and the interlayer separation, any static or dynamic correlation function can be obtained. The quantities of interest in this study are the intralayer pair correlation function $g_{11}(r)$, its Fourier transform $S_{11}(q)$ and the mean-square displacement $\langle \Delta r^2(t) \rangle$ from which the diffusion coefficient D was obtained. All of these quantities can be obtained from the position vector data set alone. The relevant formulae are

$$g_{11}(r) = \frac{\langle n(r) \rangle}{2\pi r \Delta r n} \tag{3}$$

$$S_{11}(q) = 1 + 2\pi n \int_0^\infty [g_{11}(r) - 1] r J_0(qr)\, \mathrm{d}r \tag{4}$$

$$\langle \Delta r^2(t) \rangle = \frac{1}{N} \left\langle \sum_{j=1}^{N} |\vec{r}_j(t) - \vec{r}_j(0)|^2 \right\rangle \tag{5}$$

$$D = \lim_{t\to\infty} \frac{\langle \Delta r^2(t) \rangle}{4t} = \lim_{t\to\infty} \frac{1}{4} \frac{\mathrm{d}}{\mathrm{d}t} \langle \Delta r^2(t) \rangle, \tag{6}$$

where $\langle n(r) \rangle$ is the average number of particles in one of the layers in an annulus of radius r and thickness Δr, centred at a given particle and J_0 is the Bessel function of order zero.

3.1. Diffusion

We have studied how the diffusion coefficient changes as the two layers are brought together from infinity, for a given value of Γ. For large values of the interlayer separation d (typically greater than 2.5, in units of the WS radius), the bilayer behaves as two independent layers and the diffusion is that of a two-dimensional OCP. As d approaches zero, it again behaves as a two-dimensional OCP, but with twice the density, and hence the diffusion coefficient must be less; the equivalent value of Γ increases by a factor of $\sqrt{2}$. Our results show that this decrease in the diffusion does not occur in a monotonic fashion, but goes through a well-defined minimum for a range of d.

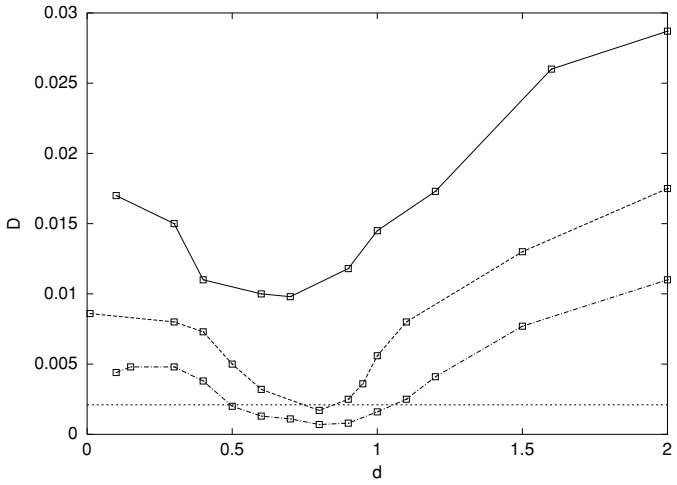

Figure 1. Dependence of diffusion coefficient D (in units of a^2/τ) on the interlayer separation d (in units of a), for various values of Γ. Solid line is for $\Gamma = 60$, dashed line for $\Gamma = 80$ and dash-dot line for $\Gamma = 100$. The horizontal line at 0.002 is the diffusion coefficient of an isolated two-dimensional OCP at freezing.

Figure 1 illustrates the variation of the diffusion coefficient D (in units of a^2/τ) with an interlayer separation d (in units of a) for some representative values of Γ. It is seen that the behaviour is the same, for any Γ with the diffusion having a minimum value for a certain d. The horizontal line indicates the diffusion coefficient of an isolated single layer at $\Gamma = 130$; experiments and MD simulations indicate a first-order fluid–solid phase transition in a two-dimensional OCP when Γ is between 120 and 140. If the same criterion is taken as an indication of a fluid–solid phase change in a bilayer, we note that a bilayer changes from a fluid to a solid and back to a fluid as the interlayer separation changes from infinity to zero. The range of d values for which the solid-like behaviour is observed depends on Γ. For Γ less than 75, the diffusion does not drop below the horizontal line for any value of d. Thus one may construct a phase diagram of a bilayer in the Γ–d plane; before doing so, we investigated other freezing signatures.

3.2. Static structure factor

A universal freezing criterion for a three-dimensional system, independent of the interaction potential [13], states that such a system freezes when $S(q_0)$, the first maximum of the static structure factor, reaches a value of 2.85. A similar analysis of two-dimensional systems with different interaction potentials [14, 15] puts this universal value around 5.0. This value is not as definite and accurate as that for three-dimensional systems, since it has been noted that $S(q_0)$ increases quite rapidly as the freezing state is approached. We have used this criterion to indicate the onset of freezing in bilayers. Figure 2 shows plots of the first maximum of the intralayer structure factor $S_{11}(q_0)$ as a function of d for some representative values of Γ.

The horizontal line is drawn at 5.2 as it is a little more consistent with our diffusion data. The states below 5.2 are then fluid states and those above are solid-like states. Here again, we note that if Γ is less than about 75, freezing does not occur for any d.

Taking the values of the diffusion coefficient (less than 0.002) and $S_{11}(q_0)$ (greater than 5.2) as equivalent signatures of freezing of a classical electronic bilayer, we have constructed a phase diagram in the Γ–d plane. This is shown in figure 3.

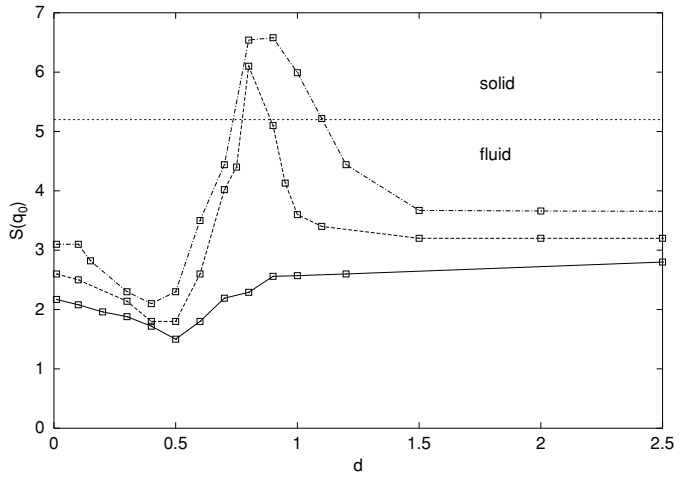

Figure 2. Amplitude of the main peak, $S_{11}(q_0)$ of the intralayer static structure factor as a function of the interlayer separation d (in units of a), for various values of Γ. Solid line is for $\Gamma = 60$, dashed line for $\Gamma = 80$ and dash-dot line for $\Gamma = 100$. The horizontal line at 5.2 is taken to be the freezing criterion of any two-dimensional system.

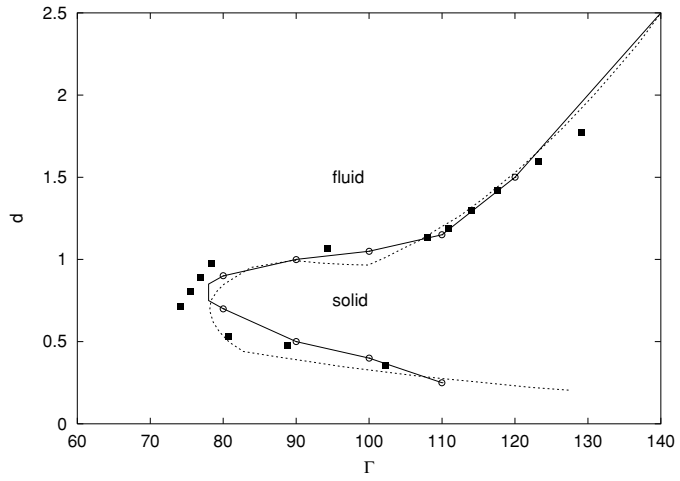

Figure 3. Phase diagram of a symmetric, classical electronic bilayer as a function of the coupling strength Γ and the interlayer separation d (in units of a). The solid line and open circle points are from our diffusion and structure factor data. The dashed line is from [10]. The closed square points are from [11].

Thus we see that a classical electronic symmetric bilayer is always in a fluid state for Γ less than about 75; however, if Γ is greater than 75 it undergoes a phase transition from a fluid to a solid for certain intermediate values of d. The larger the Γ, the larger is the range of d for which the bilayer is in a solid state. Of course, for Γ greater than 140, it is in a solid state for any d.

We have compared our phase diagram with similar graphs from [10, 11]. While a comparison with [11] is straightforward, we had to make some assumptions when it came

to [10]. In [10], the abscissa is in terms of $r_s = \frac{a}{a_B}$ (not Γ), where a_B is an *effective* Bohr radius. The relationship between Γ and r_s cannot be uniquely defined; however, it has been stated [16] that a two-dimensional OCP crystallizes at $r_s = 34 \pm 4$, while the accepted value in terms of Γ is between 120 and 140. If we further assume that the relation between Γ and r_s is linear and constant, the ratio then is between 3.2 and 4.7. The value of 4.2 produced a good agreement between the two graphs. Our system and that in [11] are classical, while a quasi-quantum bilayer with spin was considered in [10].

4. Conclusions

We have established the phase diagram of a classical, symmetric bilayer in the Γ–d plane by analysing the diffusion coefficients. We have also investigated the peak values of the intralayer static structure factor as functions of Γ and d, to arrive at a consistent picture of the phase diagram. The equivalent signatures of freezing are that the diffusion coefficient (in dimensionless units) be less than 0.002 or the amplitude of the main peak, $S_{11}(q_0)$ of the intralayer structure factor be greater than 5.2. The value of 5.2 is consistent with the values obtained for other two-dimensional systems and seems to confirm the universality of a freezing criterion. It is to be noted that our conclusions are consistent with the peak positions of the intralayer pair correlation function $g_{11}(r)$ coinciding with those of a square lattice and a pronounced square lattice structure in a typical snapshot of particle positions. It is gratifying to note that our phase diagram and those in [10] and [11] are very similar, even though the approaches to obtain it are very different.

Acknowledgment

This project was supported in part by a grant from the Academic Research Program (ARP) of the Department of National Defence, Canada.

References

[1] Mitchell T B, Bollinger J J, Dubin D H E, Huang X-P, Itano W M and Boughman R H 1998 *Science* **282** 1290
[2] Kainth D S, Richards D, Bhatti A S, Hughes H P, Simmons M Y and Ritchie D A 1999 *Phys. Rev.* B **59** 2095
[3] Liu L, Swierkowski L, Neilson D and Szymanski J 1996 *Phys. Rev.* B **53** 7923
[4] Golden K I and Kalman G 2003 *J. Phys. A: Math. Gen.* **36** 5865
[5] Donko Z and Kalman G J 2001 *Phys. Rev.* E **63** 061504
[6] Ranganathan S, Johnson R E and Pathak K N 2002 *Phys. Rev.* E **65** 051203
[7] Ranganathan S and Johnson R E 2003 *Phys. Rev.* E **67** 041201
[8] Donko Z, Hartmann P, Kalman G J and Golden K I 2003 *J. Phys. A: Math. Gen.* **36** 5877
[9] Ranganathan S and Johnson R E 2004 *Phys. Rev.* B **69** 085310
[10] Senatore G, Rapisarda F and Conti S 1999 *Int. J. Mod. Phys.* **13** 479
[11] Schweigert I V, Schweigert V A and Peeters F M 1999 *Phys. Rev. Lett.* **82** 5293
[12] Johnson R E and Ranganathan S 2001 *Phys. Rev.* E **63** 056703
[13] Hansen J P and Verlet L 1969 *Phys. Rev.* **184** 151
[14] Gann R C, Chakravarthy S and Chester G V 1979 *Phys. Rev.* B **20** 316
[15] Broughton J Q, Gilmer G H and Weeks J D 1982 *Phys. Rev.* B **25** 4651
[16] Rapisarda F and Senatore G 1996 *Aust. J. Phys.* **49** 161